Chemical Physics Letters 494 (2010) 249–254

Contents lists available at ScienceDirect

Chemical Physics Letters

journal homepage: www.elsevier.com/locate/cplett

Seed-mediated synthesis of Pd–Rh bimetallic nanodendrites

Hirokazu Kobayashi [a], Byungkwon Lim [a,*], Jinguo Wang [b], Pedro H.C. Camargo [a], Taekyung Yu [a], Moon J. Kim [b], Younan Xia [a,**]

[a] Department of Biomedical Engineering, Washington University, St. Louis, MO 63130, United States
[b] Department of Materials Science, University of Texas at Dallas, Richardson, TX 75083, United States

ARTICLE INFO

Article history:
Received 18 March 2010
In final form 3 June 2010
Available online 8 June 2010

ABSTRACT

This Letter describes a simple, aqueous-phase route to the synthesis of Pd–Rh bimetallic nanodendrites consisting of Rh branches anchored to a Pd nanocrystal core. Palladium nanocrystals with various shapes, including truncated octahedron, cube, octahedron, and thin plate, have all been successfully employed as seeds to grow Rh branches via the reduction of Na_3RhCl_6 with L-ascorbic acid in an aqueous solution. The degree of Rh branching could be controlled by varying the concentration of Na_3RhCl_6 involved in a synthesis. Electron microscopy analysis revealed that growth of Rh branches proceeded via attachment of small Rh particles that had been formed via homogeneous nucleation in solution.

1. Introduction

Rhodium is a key catalyst invaluable to many reactions, including hydrogenation, hydroformylation, carbonylation, and reduction of nitrogen oxides in a catalytic converter [1–4]. Meanwhile, Pd has been widely used to catalyze hydrogenation or dehydrogenation, carbon–carbon bond forming reactions, petroleum cracking, and formic acid oxidation [5–7]. Recently, a new type of bimetallic nanostructure, so-called 'bimetallic nanodendrite', has been prepared by a heterogeneous, seeded growth method, and has attracted intensive attention as a highly active catalyst for chemical or electrochemical reactions [8–11]. For instance, Eichhorn and co-workers prepared Au–Pt nanodendrites, which showed the enhanced CO tolerance in the hydrogen oxidation reaction in a proton-exchange membrane (PEM) fuel cell [8]. Recently, our group reported the synthesis of Pd–Pt nanodendrites, which displayed a substantially enhanced activity for the oxygen reduction and formic acid oxidation reactions in a PEM fuel cell [9,11]. However, bimetallic nanodendrites prepared so far have been restricted to those consisting of Pt branches supported on Au or Pd nanocrystal seeds. The synthesis of bimetallic nanodendrites with a wide variety of compositions remains a challenge.

Both Pd and Rh are noble metals that crystallize with a face-centered cubic (*fcc*) packing, and these two metals have a lattice mismatch of only 2.3%. Recently, Pd nanocrystals have been prepared in a rich variety of shapes, including truncated octahedron, cube, octahedron, and thin plate [12–14], making them ideal candidate as the seeds for heterogeneous, seeded growth of bimetallic nanostructures. Here we describe a simple, aqueous-phase route to the synthesis of Pd–Rh bimetallic nanodendrites consisting of Rh branches anchored to a core of Pd nanocrystal with different shapes, including truncated octahedron, cube, octahedron, and thin plate. Our synthetic protocol simply involves the reduction of Na_3RhCl_6 by L-ascorbic acid in the presence of Pd nanocrystal seeds in an aqueous solution. Using this simple approach, we were able to produce Pd–Rh nanodendrites in high yields. We also investigated the growth mechanism and found that particle attachment played an important role in the formation of a branched morphology.

2. Experimental

2.1. Preparation of Pd nanocrystal seeds with different shapes

Palladium nanocrystals used as seeds were prepared in aqueous solutions, as reported previously [13]. Palladium nanocrystals with a truncated octahedral shape were synthesized by heating 11 mL of an aqueous solution containing poly(vinyl pyrrolidone) (PVP, 105 mg, MW = 55 000, Aldrich), L-ascorbic acid (60 mg, Aldrich), citric acid (60 mg, Fisher), and Na_2PdCl_4 (57 mg, Aldrich) at 100 °C in air under magnetic stirring for 3 h. Palladium nanocrystals with a cubic shape were synthesized by heating 11 mL of an aqueous solution containing PVP (105 mg), L-ascorbic acid (60 mg), KBr (300 mg, Fisher), and Na_2PdCl_4 (57 mg) at 80 °C in air under magnetic stirring for 3 h. Palladium nanocrystals with an octahedral shape were synthesized by heating 11 mL of an aqueous solution containing PVP (105 mg), citric acid (60 mg), and Na_2PdCl_4 (57 mg,) at 90 °C in air under magnetic stirring for 26 h. Palladium nanoplates with a hexagonal or triangular shape were synthesized by heating 11 mL of an aqueous solution con-

* Corresponding author.
** Corresponding author.
E-mail addresses: limb@seas.wustl.edu (B. Lim), xia@biomed.wustl.edu (Y. Xia).

0009-2614/$ - see front matter © 2010 Elsevier B.V. All rights reserved.
doi:10.1016/j.cplett.2010.06.009

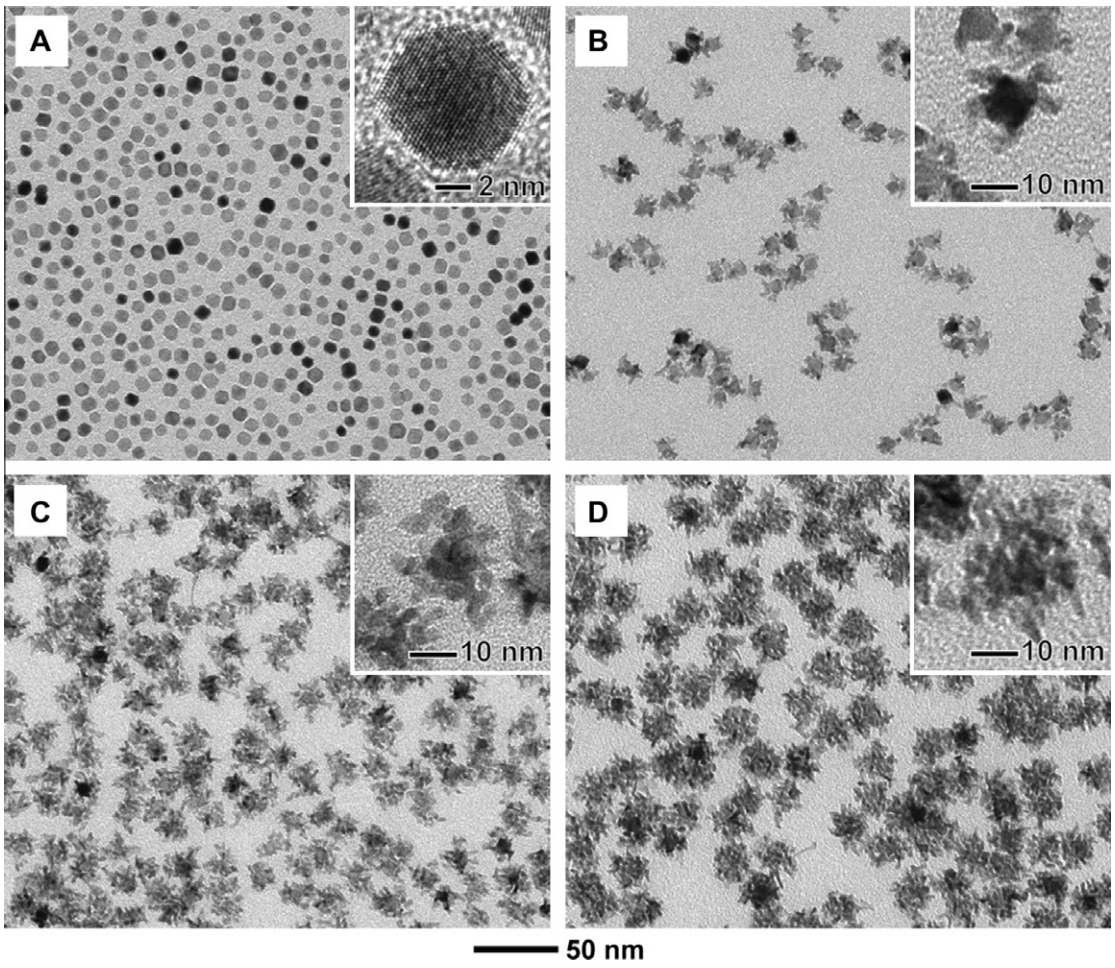

Fig. 1. (A) TEM image of truncated octahedral Pd nanocrystals used as the seeds. The inset shows an HRTEM image of a single Pd truncated octahedron. (B–D) TEM images of Pd–Rh nanodendrites synthesized by reducing Na_3RhCl_6 with L-ascorbic acid in the presence of the truncated octahedral Pd seeds in an aqueous solution. The concentration of Na_3RhCl_6 was (B) 1.6, (C) 3.2, and (D) 6.4 mM, and the reaction time was 3 h.

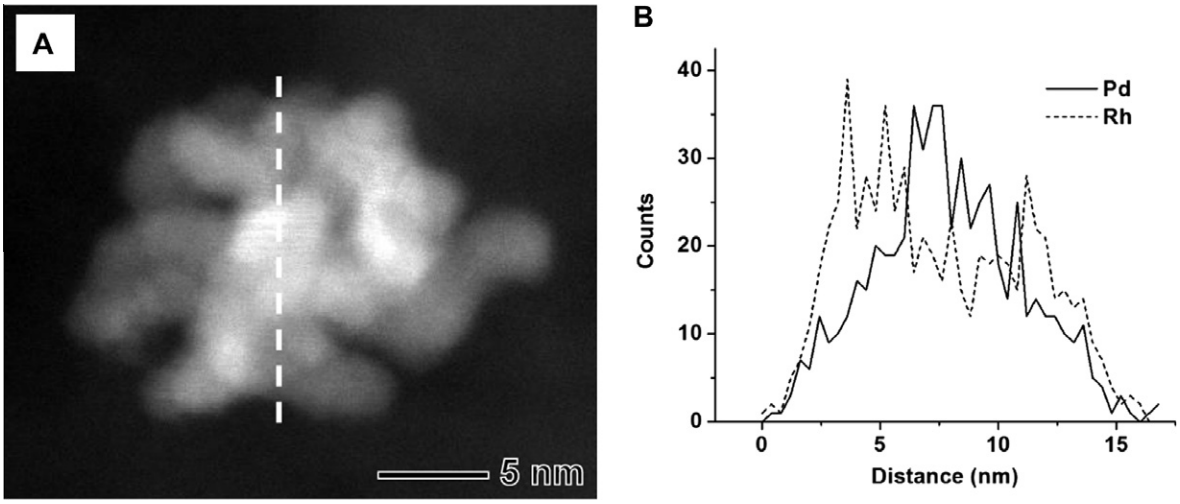

Fig. 2. (A) HAADF-STEM image of a single Pd–Rh nanodendrite shown in Fig. 1D. (B) Compositional line profiles of Pd and Ph on the Pd–Rh nanodendrite recorded along the line shown in the HAADF-STEM image.

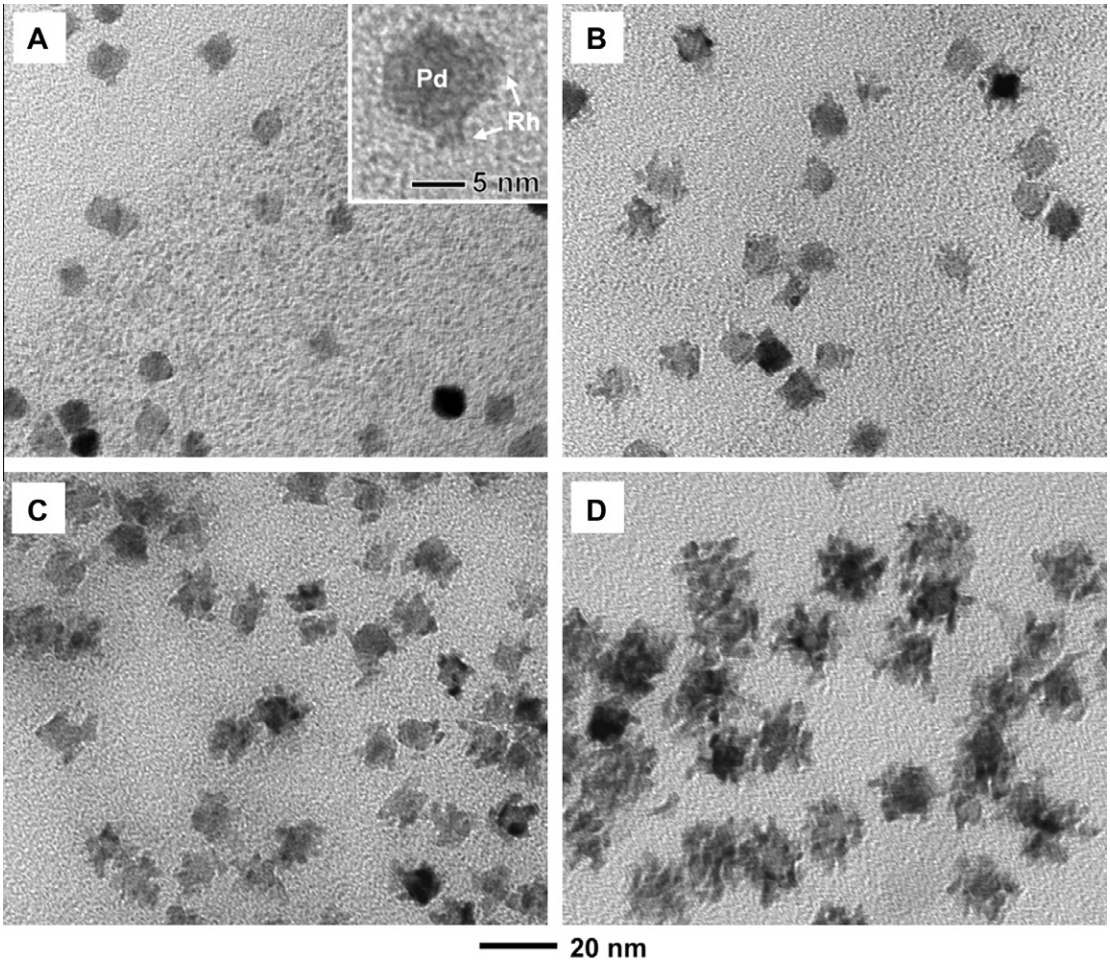

Fig. 3. TEM images showing the morphological evolution of Pd–Rh nanodendrites. The reaction was conducted under the same conditions as those in Fig. 1D except that the reaction time was shortened to (A) 1, (B) 1.5, (C) 2, and (D) 10 min. The inset of (A) shows a TEM image of a single Pd–Rh particle consisting of Rh bumps on the Pd core.

taining PVP (105 mg) and Na_2PdCl_4 (57 mg) at 100 °C in air under magnetic stirring for 3 h. These Pd nanocrystals were washed with deionized water three times before being used as seeds.

2.2. Synthesis of Pd–Rh bimetallic nanodendrites

In a typical synthesis of Pd–Rh nanodendrites, 1 mL of the aqueous suspension of Pd nanocrystals and 6 mL of an aqueous solution containing PVP (35 mg) and L-ascorbic acid (60 mg) were added into a 25-mL, three-necked flask. The mixture was heated to 100 °C in air under magnetic stirring. Meanwhile, a known amount of sodium hexachlororhodate(III) (Na_3RhCl_6, 6.3–25 mg, Aldrich) was dissolved in 3 mL of deionized water at room temperature. The aqueous solution of Na_3RhCl_6 was then injected into the flask by pipette. The reaction mixture was heated at 100 °C in air for 3 h, and then cooled down to room temperature.

2.3. Characterization

Transmission electron microscopy (TEM) images were obtained with a FEI Tecnai G2 Spirit microscope operated at 120 kV by drop casting the nanoparticle dispersions on carbon-coated copper grids. High-resolution TEM (HRTEM), high-angle annular dark-field scanning TEM (HAADF-STEM), and energy dispersive X-ray (EDS) analyses were performed using a JEOL 2100F microscope operated at an accelerating voltage of 200 kV.

3. Results and discussion

We first employed truncated octahedral Pd nanocrystals with an average size of ~9 nm as the seeds for the formation of Pd–Rh bimetallic nanodendrites. A TEM image of the as-prepared Pd truncated octahedrons shows that they were uniform in both shape and size (Fig. 1A). An HRTEM image of a single Pd truncated octahedron indicates that it was a piece of single crystal with its surface being enclosed by both {1 1 1} and {1 0 0} facets (Fig. 1A, inset). The Pd–Rh nanodendrites were synthesized in an aqueous solution by reducing Na_3RhCl_6 with L-ascorbic acid as a reducing agent in the presence of truncated octahedral Pd seeds. Fig. 1B–D, shows typical TEM images of the products prepared with different concentrations of Na_3RhCl_6. In all cases, Rh grew into branches on the Pd seeds, generating Pd–Rh bimetallic nanocrystals with an overall dendritic morphology. The compositional line profiles (Fig. 2) of Pd and Rh on a Pd–Rh nanodendrite shown in Fig. 1D confirmed its bimetallic composition consisting of a Pd core and Rh branches. For the sample prepared at a relatively low concentration for the Na_3RhCl_6 precursor, each Pd–Rh nanodendrite had very few (5–10) branches, and most of them remained single branches (Fig. 1B). As the Na_3RhCl_6 concentration was increased, the number of Rh branches increased, and secondary branching was also observed. These results demonstrate that the degree of Rh branching can be readily controlled by varying the concentration of the Na_3RhCl_6 precursor involved in a synthesis. The TEM

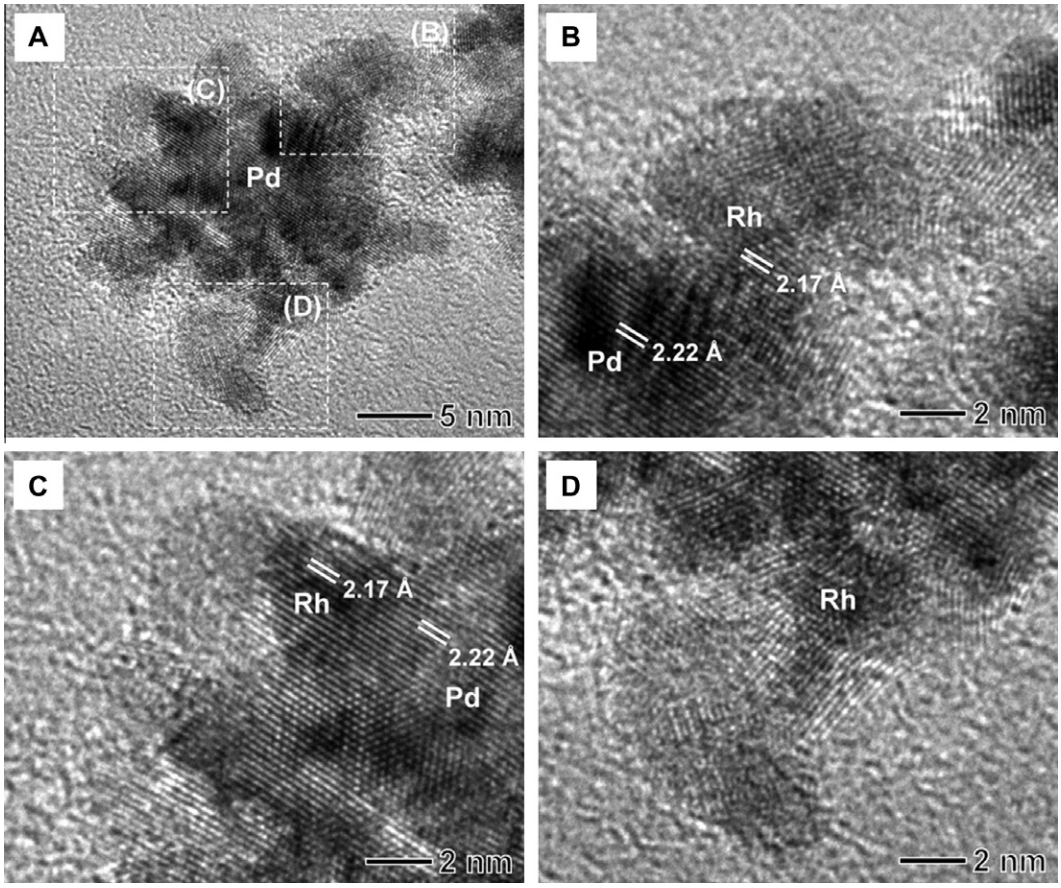

Fig. 4. (A) HRTEM image of a single Pd–Rh nanodendrite. (B–D) Magnified HRTEM images of the boxed regions in (A). The images reveal that the Rh branches have the same lattice orientation as the Pd core at the interfaces, but the lattice fringes are not perfectly aligned across all the branches.

analysis confirmed the absence of isolated Rh nanoparticles in the product.

We investigated the morphological evolution of the Pd–Rh nanodendrites by taking aliquots of the reaction solution at various stages and then viewing them by electron microscopy. The reaction was conducted at a relatively high concentration of Na_3RhCl_6 (see Fig. 1D). Fig. 3A–D, shows typical TEM images of the Pd–Rh nanostructures that were sampled at 1, 1.5, 2, and 10 min, respectively. At $t = 1$ min, the Pd–Rh sample contained small Rh particles with sizes less than 3 nm in great abundance in addition to some Rh-decorated Pd seeds (Fig. 3A). This observation suggests that homogeneous nucleation of Rh occurred in the solution, as well as heterogeneous nucleation on the surface of the Pd nanocrystal seeds. The image in the inset of Fig. 3A clearly shows the formation of Rh bumps via heterogeneous nucleation on the Pd seed. As the reaction proceeded, the number of small Rh particles rapidly decreased while Rh branches on each Pd seed increased in both number and size (Fig. 3B and C), indicating that the Rh branches were formed through attachment of small Rh particles. The Pd–Rh particles eventually evolved into a highly branched structure through the digestion of essentially all the small Rh particles (Fig. 3D).

Fig. 4A displays an HRTEM image of one of the Pd–Rh nanodendrites shown in Fig. 1D, which shows that the surface of the Pd core was almost covered by a number of Rh branches. The Rh branches had an average diameter of ~3 nm. The HRTEM images in Fig. 4B and C, reveal the continuous lattice fringes from the Pd core to the Rh branches at the interfaces, indicating that the Rh bumps were grown epitaxially on the Pd seed (note that Pd and Rh only have a lattice mismatch of 2.3%). For the Rh branches, however, lattice fringes were not aligned across the entire branches, suggesting that the Rh particles were randomly fused into the Rh bumps nucleated on the Pd seed and the growing Rh branches (Fig. 4B and D).

In this synthesis, the formation of small Rh particles at the early stages of the reaction can probably be attributed to the rapid increase in the degree of supersaturation for Rh atoms due to the fast reduction of Na_3RhCl_6 precursor by L-ascorbic acid. It is known that a higher degree of supersaturation can facilitate the homogeneous nucleation in a solution. The attachment of small Rh particles may be driven by their high energy due to a large surface area-to-volume ratio [15,16]. In previous studies of seeded growth of bimetallic nanodendrites [8–10], nanocrystals were considered to grow by heterogeneous nucleation and subsequent growth by atomic addition. Our results clearly show that both homogeneous and heterogeneous nucleation of Rh occurred at the very early stages of the synthesis and the Rh branches grew via particle attachment. This kind of nanocrystal growth has also been observed in the synthesis of Pd–Pt nanodendrites [11].

Palladium nanocrystals with different shapes were also evaluated as seeds to direct the dendritic growth of Rh branches. Fig. 5A–C, shows TEM images of Pd nanocrystals with cubic, octahedral, and plate-like morphologies, respectively. The cubic and octahedral nanocrystals are enclosed by the {1 0 0} and the {1 1 1} facets, respectively, while the thin plates with a triangular or hexagonal shape are covered by the {1 1 1} facets on their top and bottom faces. Fig. 5D and E, shows TEM images of Pd–Rh nanocrystals prepared with the cubic and octahedral Pd nanocrystals as the seeds, respectively. In both cases, the products exhibited a morphology similar to that of the Pd–Rh nanodendrites obtained from the truncated octahedral Pd seeds shown in Fig. 1D. Interest-

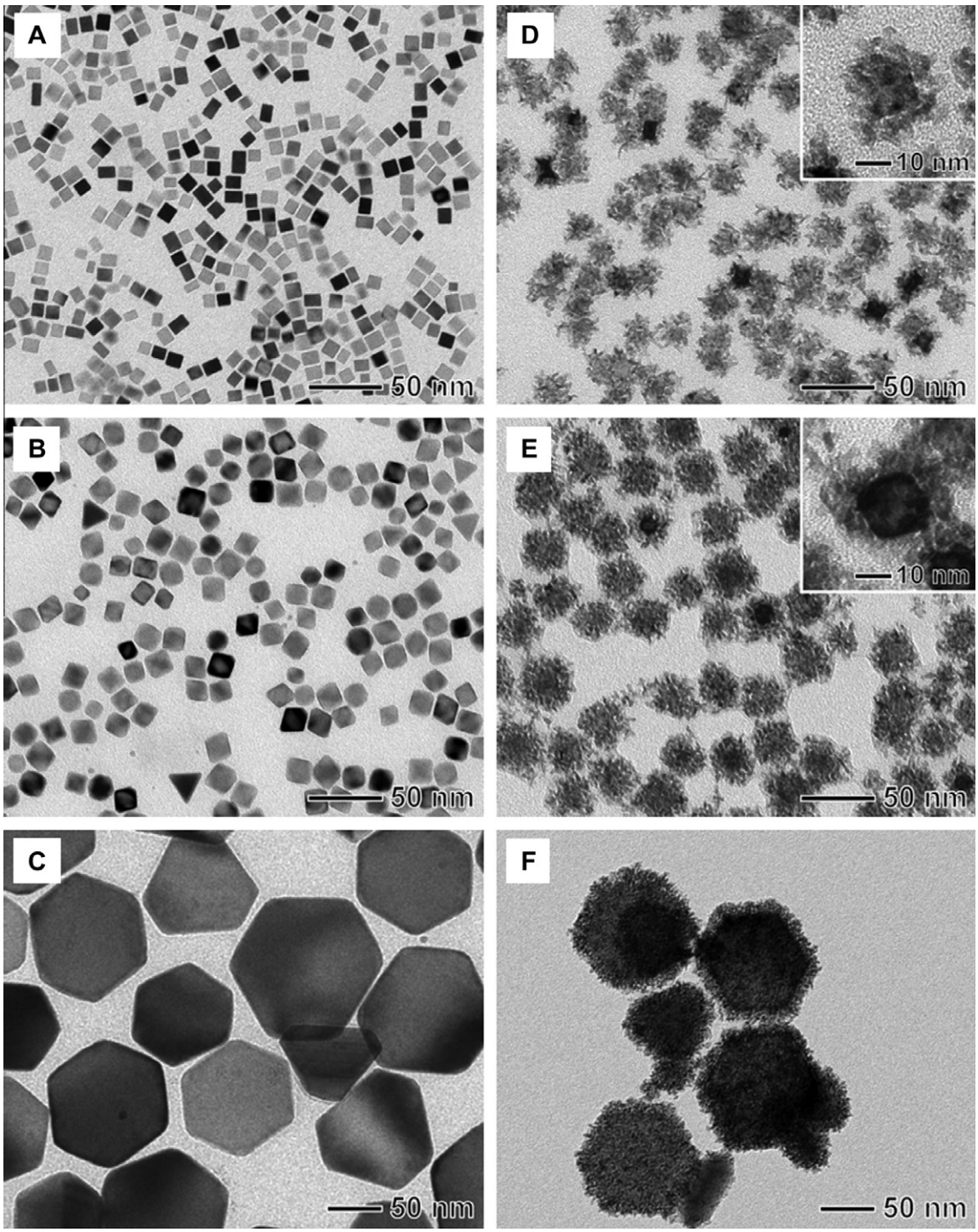

Fig. 5. (A–C) TEM images of Pd nanocrystals with cubic, octahedral, and plate-like morphologies, respectively. (D–F) TEM images of Pd–Rh bimetallic nanocrystals grown on the Pd seeds shown in (A–C), respectively. In each case, the synthesis was conducted by reducing Na_3RhCl_6 with L-ascorbic acid in the presence of Pd seeds in an aqueous solution.

ingly, the use of Pd nanoplates as seeds resulted in the formation of an unconventional nanostructure consisting of a dense array of Rh branches that were distributed more or less evenly over the entire surface of a Pd nanoplate core (Fig. 5F). These results indicate that growth of Rh branches is essentially independent of the facets expressed on the surface of the Pd nanocrystals used as the seeds, and suggest that our approach can be considered as a general route to the synthesis of Pd–Rh bimetallic nanodendrites.

4. Summary

We have demonstrated the synthesis of Pd–Rh bimetallic nanodendrites consisting of a dense array of Rh branches supported on a Pd nanocrystal core via a simple, aqueous-phase route. We have shown that both homogeneous and heterogeneous nucleation of Rh occurred at the very early stages of the synthesis and the growth of Rh branches proceeded via particle attachment. The de-

gree of Rh branching could be controlled by varying the concentration of a Na_3RhCl_6 precursor involved in a synthesis. Combining the properties of both Pd and Rh, the Pd–Rh bimetallic nanodendrites hold great potential for fundamental studies of the catalytic properties. This synthetic strategy based on seeded growth could also be extended to other bimetallic systems such as Pt–Rh.

Acknowledgements

This work was supported in part by the NSF (DMR-0804088) and startup funds from Washington University. J.W. was supported by a grant from CNMT (08K1501-01 210) under the 21st Frontier R&D Program of the MEST, Korea. P.H.C.C. was also partially supported by the Fulbright Program and the Brazilian Ministry of Education (CAPES). T.Y. was also partially supported by the National Research Foundation of Korea (NRF-2009-352-D00160). Part of the work was performed at the Nano Research Facility (NRF), a member of the National Nanotechnology Infrastructure Network (NNIN), which is supported by the National Science Foundation under award ECS-0335765.

References

[1] P.N. Rylander, Hydrogenation Methods, Academic Press, New York, 1985.
[2] W.M. Pearlman, Org. Synth. Coll. 5 (1973) 670.
[3] M. Fujita, T. Hiyama, Org. Synth. Coll. 8 (1993) 16.
[4] A. Akao, K. Sato, N. Nonoyama, T. Mase, N. Yasuda, Tetrahedron Lett. 47 (2006) 969.
[5] M. Fernandez-Garcia, A. Martinez-Arias, L.N. Salamanca, J.M. Coronado, J.A. Anderson, J.C. Conesa, J. Soria, J. Catal. 187 (1999) 474.
[6] Y. Nishihata et al., Nature 418 (2002) 164.
[7] J.M. Thomas, B.F.G. Johnson, R. Raja, G. Sankar, P.A. Midgley, Acc. Chem. Res. 36 (2003) 20.
[8] S. Zhou, K. McIlwrath, G. Jackson, B. Eichhorn, J. Am. Chem. Soc. 128 (2006) 1780.
[9] B. Lim et al., Science 324 (2009) 1302.
[10] Z. Peng, H. Yang, J. Am. Chem. Soc. 131 (2009) 7542.
[11] B. Lim, M. Jiang, T. Yu, P.H.C. Camargo, Y. Xia, Nano Res. 3 (2010) 69.
[12] B. Lim, Y. Xiong, Y. Xia, Angew. Chem. Int. Ed. 46 (2007) 9279.
[13] B. Lim, M. Jiang, J. Tao, P.H.C. Camargo, Y. Zhu, Y. Xia, Adv. Funct. Mater. 19 (2009) 189.
[14] B. Lim, H. Kobayashi, P.H.C. Camargo, L.F. Allard, J. Liu, Y. Xia, Nano Res. 3 (2010) 180.
[15] H. Zheng, R.K. Smith, Y.-w. Jun, C. Kisielowski, U. Dahmen, A.P. Alivisatos, Science 324 (2009) 1309.
[16] B. Lim, J. Wang, P.H.C. Camargo, C.M. Cobley, M.J. Kim, Y. Xia, Angew. Chem. Int. Ed. 48 (2009) 6304.